ISBN: 978-3-95450-223-3 ISSN: 2673-7000 doi:10.18429/JACoW-NAPAC2019-MOYBA1

LHC STATUS AND PLANS

X. Buffat, CERN, Geneva, Switzerland

Abstract

Performance and accelerator physics challenges from LHC Run 2 are reviewed, along with the ongoing preparation and plans for LHC Run 3 and beyond.

INTRODUCTION

The Large Hadron Collider (LHC) [1] features two high energy hadron beams steered by superconducting magnets on circular trajectories of about 27 km. Those beams circulate with opposite directions in separate beam pipes and collide with a high rate at the centre of four detectors at distinct locations around the ring. As illustrated in Fig. 1, the first run of the LHC featured a maximum energy 4 TeV per beam. Following the consolidation of the splices of the main dipoles' superconducting busbars during the first Long Shut down (LS1) [2], the machine could be restarted for a second run at an energy of 6.5 TeV, just below the design energy of 7 TeV. The first section is dedicated to the performance of the LHC during its second run while the second section describes its High Luminosity upgrade, the HL-LHC [3], including the tests of some technologies performed during run 2. Eventually, some considerations about the challenges for the third run of the LHC will be discussed in the last section.

RUN 2

Figure 2 shows the peak luminosity achieved during run 2 of the LHC. The first year was dedicated to the recovery from the LS1 down with emphasis on high energy operation with a large number of bunches, i.e. with a 25 ns spacing between the bunches, enhancing electron cloud effects [4]. β^* and crossing angle were reduced in 2017 thus approaching the limit imposed by the physical aperture of the triplet and long-range beam-beam interactions as illustrated by Fig. 3. In this configuration the design luminosity could be exceeded. The β^* was further reduced in 2017 profiting from the experience acquired with the limits imposed by the non-linearities of the forces that the two beams exert on each other in the common chamber around each experiment, the so-called long-range beam-beam interactions [5]. Additionally, dynamic changes of the crossing angle during data acquisition phases were introduced to follow the relaxation of the limits as the beam intensity decays [6]. This strategy was further pushed in 2018 by reducing the β^* while the beams are colliding [7]. Not only these complex operational procedures improved the integrated luminosity by some percent, they also constitute valuable experience for the HL-LHC whose operational scenario is based on β^* levelling [3].

To achieve the low operational β^* of 30 to 25 cm, the Achromatic Telescopic Squeeze (ATS) [8] was used with a telescopic index of 1.3 to 1.6. An optics featuring a telescopic index of 3.1, corresponding to the HL-LHC baseline [3], was tested in dedicated experiments with high intensity beams. The correctability of this optics could be demonstrated as well as additional benefits including the enhancement of the effective strength of the arc octupole for Landau damping as well as for global compensation of long-range beam-beam effects [9].

The correction of the non-linear aberrations of the final focusing magnets became unavoidable for operation with β^* lower than 40 cm as their impact on the amplitude detuning, and consequently Landau damping, became significant. Additionally, the accuracy of the β^* was affected to a level that an imbalance could be detected in the luminosity delivered to the two main experiments [10]. A combination of K-modulation and AC-dipole measurements are used to obtain the required accuracy in the linear and non-linear optics correction [10, 11].

The energy stored in each beam reached 320 MJ during run 2. The sensitive equipment are protected from particle losses by a hierarchy of collimators. For both safe and efficient usage of the physical aperture, the collimators are placed as close to the beam as possible, yet respecting the hierarchy which is critical to maintain the efficiency of this multistage cleaning scheme. This imposes tight constraints on the orbit and optics correction, as well as its stability [12]. Efficient alignment and validation procedures were implemented to ensure the robustness of the operation with minimum commissioning time, e.g. the time dedicated to alignment was reduced from 20 hours to 30 minutes thanks to the implementation of BPM embedded in the collimator jaws and the usage of fully automated procedure [13]. The tightening of the collimation hierarchy improved the fraction of proton lost outside of the designated areas, i.e. the cleaning inefficiency, down to 10^{-4} which is a factor 6 lower than design [14]. The corresponding increase of the transverse impedance along with the reduction of the Landau damping generated by the octupoles at a higher energy makes the beam stability significantly more critical with respect to the first run of the LHC at 4 TeV. Nevertheless the brightness limit arising from transverse instabilities observed in run 1 [15, 16] was lifted mostly by the significant improvements in the control of linear coupling [17, 18] and by the improved controls of non-linearities above mentioned.

A significant fraction of the achievements in term of luminosity at the LHC can be attributed to the performance of its injectors, providing bunch trains with a 25 ns longitudinal spacing with transverse emittances more than twice as low as estimated at the design stage for the same intensity [19]. The brightest beam based on the Batch Compression Merging and Splitting (BCMS) [20] in the PS features slightly less bunches per train, 48 instead of 72. Consequently the total

ISBN: 978-3-95450-223-3 ISSN: 2673-7000 doi:10.18429/JACoW-NAPAC2019-MOYBA1

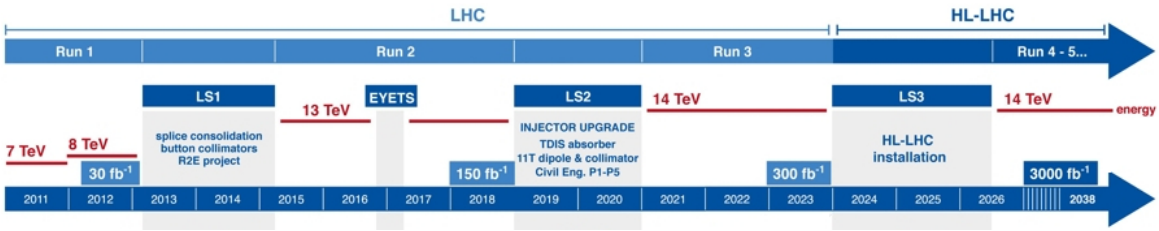

Figure 1: LHC and HL-LHC schedule. Courtesy [3].

number of bunches in the LHC was 2556, i.e. slightly below the design value of 2808.

By identifying and mitigating significant causes of down time such as the radiation to sensitive equipment [21], as well as by optimising operational procedures for example with the combination of the energy ramp and the squeeze [22], the time spent in data taking reached about 50% during the production years of run 2 [23]. The integrated luminosity delivered with protons to the high luminosity experiments ATLAS and CMS exceeded slightly the target, reaching 160 fb^{-1} [24, 25]. 6.7 fb^{-1} and 3.3 pb^{-1} were delivered to the other two experiments respectively LHCb and ALICE [24, 25].

The proton run was significantly affected by an air inlet in the pipe that occurred during the cool down of sector 12 [26], which was warmed up to exchange a faulty dipole magnet [27]. As a result, the air froze on the beam pipe and macro-particles of this condensate occasionally reached the beam trajectory, in a similar manner as the Unidentified Falling Objects (UFO) discovered in the LHC during its first run. The macro-particles of condensate release at 16L2 have a significantly lower sublimation temperature with respect to regular UFOs. Whereas the normal behaviour results in the repulsion of the solid macro-particles, the 16L2 condensates rapidly sublimate and gets ionised, resulting in a high local density of ions and electrons with balanced space charge forces [28, 29]. The ions and electrons resulted respectively in local beam losses (Fig. 4) and the development of a coherent instability with a rise time reaching 10 [30]. It was found that the field of neighbouring orbit correctors effectively reduced the frequency of these UFO-like events suggesting that local generation of electron clouds by the beam passage played a role in the mechanism of release of the macro-particles [26]. Consequently the so-called 8b4e scheme [31], featuring electron cloud clearing gaps of 4 empty slots every 8 bunch, was used for the second half of

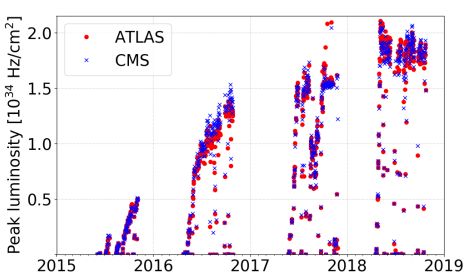

Figure 2: Peak luminosity with protons during run 2 [25]

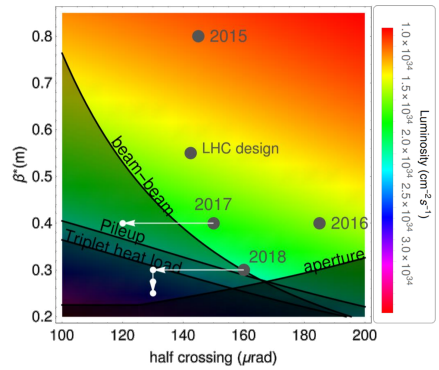

Figure 3: Estimated peak luminosity for the LHC in 2018 as a function of β^* and crossing angle at the two high luminosity experiments (color coded). The constraints are marked with black lines. The settings at start of collision for the different years are marked with grey dots, the white lines describe the dynamic changes of crossing angle and β^* as the beams intensity decay during the fill. Courtesy [7]

the year. Additionally, a warm solenoid was installed around the 16L2 interconnect already in 2017 with the aim of reducing locally the multipacting and consequently the frequency of the events [26]. The latter was reduced even further by a partial warm up of sector 12 during the year-end technical stop such that the BCMS scheme could be used again for the last year of run 2. Nevertheless the bunch intensity seemed limited at around $1.2 \cdot 10^{11}$ p per bunch.

Another non-conformity was observed in the form of an unexpected aperture restriction at the arc cell 15R8, known as the Unidentified Lying Object (ULO). The implementation of a local orbit bump was sufficient to avoid any detrimental impact on the performance during run 2. Nevertheless the object was removed during the present long shutdown and could be identified as a piece of plastic likely coming from the former wrapping of the beam screen which would have been ripped off during installation [32].

While most of the operation time was dedicated to low-β proton physics, a series of special runs took place. Forward physics studies were performed with β^* up to 2.5 km at 6.5 TeV and β^* of 90 m at the injection energy of 450 GeV [33]. An important improvement in the suppression of the background was obtained in this condition using a novel collimation scheme based on crystal channelling [14].

The peak luminosity with fully stripped lead ions at 6.37 Z TeV exceeded by a factor 6 the design value of 10^{27} Hz/cm^2 [34]. This required major improvements in the ion injector chain to provide more intense ion bunches

ISBN: 978-3-95450-223-3 ISSN: 2673-7000 doi:10.18429/JACoW-NAPAC2019-MOYBA1

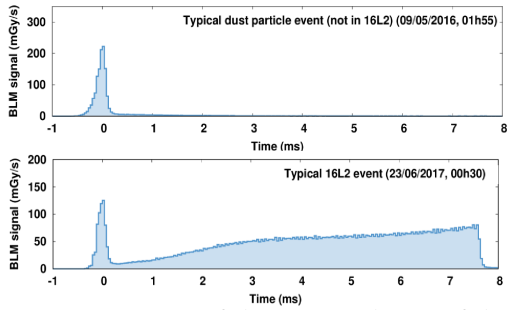

Figure 4: Comparison of the time evolution of the local losses generated by a standard UFO and a 16L2 event. Courtesy [28]

with a reduced longitudinal spacing as well as the mitigation of the losses due to Bound-Free Pair Production (BFPP) at the two main IPs with dedicated orbit bumps guiding the resulting ions bound with a single electron away from cold areas [34, 35].

The ion program was complemented with a reference proton run with a beam energy corresponding to the energy per nucleon in the lead ion run, i.e. 2.51 TeV, as well as a proton-lead run at 4 Z TeV [35, 36]. The latter could be realised in spite of the two-in-one design of the LHC magnets. A short run with fully stripped Xenon ions was realised [34]. A major step was taken towards the applications of high energy partially stripped ions [37, 38] with a first energy ramp to 6.5 TeV of $^{208}Pb^{81+}$ ions [39]. The main limitation arising from the stripping of electrons at the primary collimators which reduces the ions' rigidity will be mitigated by the additional collimator planned in the dispersion suppressor in the frame of the HL-LHC project [40].

THE HIGH-LUMINOSITY LHC

The High-Luminosity upgrade of the LHC aims at delivering 3000 fb^{-1} in the two high luminosity experiments while maintaining the data quality by limiting the pile up [3]. This is achieved mainly through an increase of the bunch intensity and a reduction of the β^*, with major consequences described in the following. The target virtual luminosity is higher than limit imposed by the maximum pile up that the experiments may tolerate after their upgrade, corresponding to 5 to 7.5·10^{34} Hz/cm^2. The luminosity will therefore be levelled at this value by adjusting β^* as the beam intensity decays.

The production of higher intensity beams requires a major upgrade of the injector chain: the LHC Injector Upgrade project (LIU) [41]. The construction of the new LINAC4, accelerating H$^-$ ions to 160 MeV, replacing the 50 MeV proton LINAC2, lifts the brightness limitation due space charge effects in the PS booster. Its extraction energy is increased from 1.4 to 2.0 GeV to mitigate space charge effects also in the PS. The RF system of the PS is consolidated in particular in terms of beam stability with the installation of a new broad-band feedback system. The SPS benefits from a RF power upgrade, a reduction of the longitudinal impedance as well as partial amorphous carbon coatings for electron cloud mitigation. A new beam dump as well as additional protection devices are also installed in the SPS to cope with the increased beam intensity and brightness. The LIU project is currently in the installation phase, the commissioning will be performed gradually through run 3, such that the full intensity can be delivered at the start of the HL-LHC project [42].

To improve the beam stability in the HL-LHC, some of the collimators based on Carbon-Fibre reinforced Carbon (CFC) will be replaced by collimators based on Molybdenum-Graphite bulk with an additional thin Molybdenum coating for the secondary collimators, featuring both a high robustness and better conductivity, thus reducing their impact on beam instabilities. First tests with beams confirmed the improvement in impedance [43]. 6 new low-impedance collimators will be installed in each beam during the LS2 [44].

The increase of off-momentum losses downstream of the betatron collimation insertion due to diffractive interactions in the primary collimator will be mitigated with the installation of an additional protection device in the dispersion suppressors for ion and proton operation. A similar scheme will be implemented downstream of the insertion hosting ALICE to cope with the increase of BFPP losses in heavy ion collisions [44]. The necessary space at the collimation insertion (IR7) is cleared by replacing an NbTi magnet featuring 8.33 T with two shorter Nb_3Sn magnets reaching 11 T [45]. Prototypes are currently under test, their installation is scheduled during the LS2. Additionally, new absorbers and protection devices will be installed in the interaction regions to cope with the increase of the luminosity and the corresponding debris [44].

In order to mitigate the increase of RF power required to compensate for transient beam loading, the HL-LHC relies on the RF full detuning scheme which was successfully implemented for operation in 2017 [46].

The effect of the strong non-linearities generated by the long-range interactions between the two beams in the common chamber around the IPs increases as the beam intensity increased and β^* decreases. As a result, a large crossing angle between the beam is required at the IP, with two major consequences. First, the physical aperture of the final focusing magnets has to increase significantly. This is addressed by replacing the inner triplet with large aperture Nb_3Sn quadrupoles [3]. Long prototypes are in the testing phase. New beam screens were designed and built, featuring tungsten shielding to mitigate the irradiation of the coils by luminosity debris and a coating with amorphous carbon [3]. The latter mitigates the electron cloud build up [47], thus limiting the local heat load as well as the detrimental effects on the beam quality visible already during run 2 [4, 48].

The geometric reduction of the luminosity due to the large crossing angle at the IP is comparable to the gain obtained with the low β^* and consequently needs to be compensated. For that purpose, 2 crab cavities will be installed on each side of the two main IPs, on each beam [3]. These cavities generate transverse deflecting electric fields with a voltage up to 3.4 MV oscillating at a frequency of 400 MHz. The

ISBN: 978-3-95450-223-3 ISSN: 2673-7000 doi:10.18429/JACoW-NAPAC2019-MOYBA1

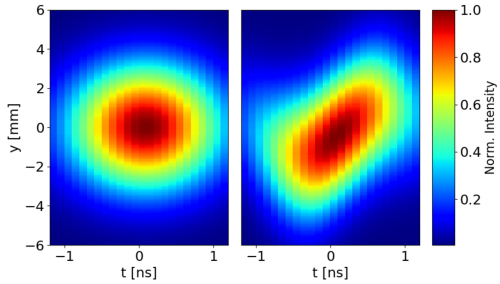

Figure 5: Transverse density profile measured as a function of time during a bunch passage through a wideband pickup for a non-crabbed (left) and crabbed (right) bunch at the SPS. Courtesy [49].

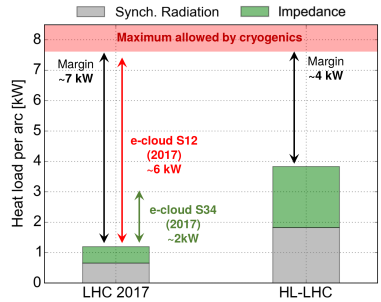

Figure 6: Comparison of the cryogenic capacity with respect to the head load generated by synchrotron radiation (gray) and RF beam induced heating (green). The difference corresponds to the margin left to cope with the head load generated by the build up of electron clouds. Courtesy [50].

phase is such that the particles at the centre of each bunch are not affected, while the ones at the head and tail are deflected in opposite directions yielding a local crab angle of up to 190 μrad at the IP thus compensating 76% of the crossing angle. They will be located between the separation dipole D2 and the first matching quadrupole Q4. To demonstrate their usability on proton beams and acquire operational experience, a test with the Double Quarter Wave (DQW) prototype was performed at the SPS, with two cavities in a single cryostat. Successful global crabbing was demonstrated through measurement with wide-band transverse pickups (Fig. 5) and several RF design, operational and beam dynamics aspects could be tested [49].

Since the existing underground facilities are not sufficient to host the new equipment in the interaction region and given the issues with radiation to equipment encountered in run 1 [21], a new powering scheme was designed. The high power equipment will be installed in a new separate radiation free cavern. Superconducting links are used to bring the power to the IR magnets [3]. Additionally, the cooling capacity is expected to become critical as discussed in the next section. A new cryogenic plant will therefore be constructed to cope with the increased load at each of the two interaction regions hosting high luminosity experiments. The cryogenic needs as well as the ventilation of the new tunnel requires a new shaft [3]. The civil engineering of these infrastructures is currently taking place, such that the corresponding HL-LHC equipment can be installed after the LHC run 3.

MAIN CHALLENGES FOR RUN 3

The injectors performance is expected to gradually reach the requirements for the HL-LHC during run 3 of the LHC [42]. The heat load on the beam screen is a particular concern for operation with higher bunch intensities [50, 51]. Indeed, during run 2 the total cooling capacity was used in some of the sectors, whereas the contributions of the beam driven RF heating as well as the synchrotron radiation are expected to be almost negligible (Fig. 6). The main load can be attributed to the building up of electron clouds due to the beam passage [4, 50]. Yet several aspects remain to be understood, in particular the apparent increase in heat load between run 1 and 2 as well as the large differences between the sectors. Several investigations of the chemical properties of the surface of the beam screen samples extracted from the magnets are currently ongoing. As shown in Fig. 6, the increase of the contribution of RF heating and synchrotron radiations with higher beam energy and intensity reduces the margin for the electron cloud contribution. Simulations and experimental studies show that the electron cloud build up feature a saturation or even a reduction for high intensity bunches [4], such that the current cryogenic capacity could remain sufficient if no further degradation of the beam screen surface occurs during LS2. New types of beams were devised for the mitigation of electron cloud build up, such as the 8b4e mentioned above, and their effectiveness was demonstrated experimentally [4]. Nevertheless these schemes feature a reduced total number of bunches in the LHC which, in a pile-up limited regime, reduce the luminosity. The usage of mixed schemes, as well as the capacity of the injector chain to efficiently provide them, was demonstrated such that they can be used to optimally use the existing cryogenic capacity [4, 50, 51].

At the end of run 2 a tests were perform to assess the training behaviour of the main dipoles (Fig. 7). To reach the energy of 7 TeV, a training campaign of approximatively 3 months, involving in the order of 600 quenches, seem necessary [52, 53]. This large amount of quenches increases the risk of shorts in the cold diodes diverting the current in case of quench. Additional insulations are currently getting installed in each of the 1232 diodes as a mitigation of this risk [54]. Moreover, as observed in Fig. 7, the extrapolations suffer large uncertainties due to the lack of data in the 6.75 to 7 TeV range. The strategy to increase the energy during the first years of run 3 is under discussion.

The luminosity limits due to the heat load on the triplet and to pile up in the detectors will not be lifted during run 3, while LIU beams allows for higher virtual luminosity [55]. The large range of β^* needed to achieve this levelling (1.5 to 0.3 m) pushes further the effort started in run 2 in terms of optics, flexibility and operational complexity. Moreover in this heavily levelled regime, the integrated luminosity is strongly affected by unexpected beam aborts during the

ISBN: 978-3-95450-223-3 ISSN: 2673-7000 doi:10.18429/JACoW-NAPAC2019-MOYBA1

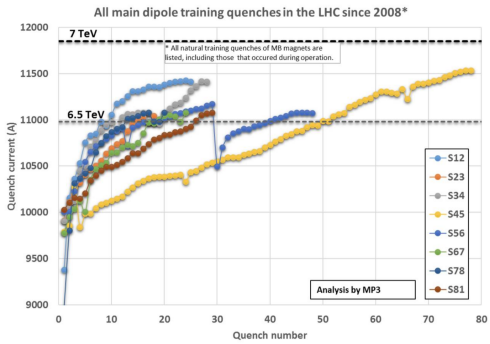

Figure 7: Maximum current reached by the various sectors in during the training campaigns since 2008. Courtesy [53].

levelling phase, the machine reliability will therefore be a key in achieving a high performance.

The triplets in the main experiments are expected to reach the end of their lifetime towards the end of run 3 due to the integrated dose received [56]. They will be replaced by larger aperture triplets for the HL-LHC.

ACKNOWLEDGEMENTS

This contribution briefly summarises selected topics about the LHC status and plans, more details can be found in the references and the achievements should be credited to the corresponding authors. Thanks to G. Arduini, P. Collier and E. Métral for proofreading it.

REFERENCES

[1] O. Brüning, *et al.*, ed., *LHC Design report*, vol. 1 : The LHC Main ring. Geneva, Switzerland: CERN, 2004.

[2] J. P. Tock, *et al.*, "Consolidation of the lhc superconducting magnets and circuits," *IEEE Trans. Appl. Supercond.*, vol. 26, pp. 1–6, June 2016.

[3] G. Apollinari, et al., *High-Luminosity Large Hadron Collider (HL-LHC): Technical Design Report V. 0.1*. CERN Yellow Reports: Monographs, Geneva: CERN, 2017.

[4] G. Iadarola, *et al.*, "Electron cloud and heat loads in run 2," in *Proc. 2019 Evian workshop on LHC beam operation*, 30 Jan.-1 Feb. 2019.

[5] X. Buffat, *et al.*, "Long-range and head-on beam-beam interactions : What are the limits ?," in *Proc. 2016 Evian workshop on LHC beam operation*, pp. 133–140, 13-15 Dec. 2016.

[6] N. Karastathis, *et al.*, "Crossing angle anti-leveling at the LHC in 2017," in *Proc. IPAC'18*, pp. 184–187, 29 April - 4 May 2018.

[7] R. Bruce, *et al.*, "Machine configuration," in *Proc. 2019 Evian workshop on LHC beam operation*, 30 Jan.-1 Feb. 2019.

[8] S. Fartoukh, "Achromatic telescopic squeezing scheme and application to the lhc and its luminosity upgrade," *Phys. Rev. ST Accel. Beams*, vol. 16, p. 111002, Nov 2013.

[9] S. Fartoukh, *et al.*, "Round telescopic optics with large telescopic index," Tech. Rep. CERN-ACC-2018-0032, CERN, Geneva, Sep 2018.

[10] E.H. Maclean, *et al.*, "New approach to LHC optics commissioning for the nonlinear era," *Phys. Rev. Accel. Beams*, vol. 22, p. 061004, Jun 2019.

[11] T. Persson, *et al.*, "LHC optics commissioning: A journey towards 1% optics control," *Phys. Rev. Accel. Beams*, vol. 20, p. 061002, Jun 2017.

[12] R. Bruce, *et al.*, "Reaching record-low β^* at the CERN large hadron collider using a novel scheme of collimator settings and optics," *Nucl. Instrum. Methods Phys. Res. A*, vol. 848, pp. 19 – 30, 2017.

[13] G. Azzopardi, *et al.*, "Operational results of the LHC collimaotr alignement using machine learning," in *Proc. IPAC'19*, pp. 1208–1211, 19-24 June 2019.

[14] N. Fuster-Martinez, *et al.*, "Run 2 collimation overview," in *Proc. 2019 Evian workshop on LHC beam operation*, 30 Jan.-1 Feb. 2019.

[15] N. Mounet, *et al.*, "Impedance and instabilities," in *Proc. 2014 Evian workshop on LHC beam operation*, pp. 59–68, 2-4 June 2014.

[16] T. Pieloni, *et al.*, "Two beam effects," in *Proc. 2014 Evian workshop on LHC beam operation*, pp. 69–80, 2-4 June 2014.

[17] T. Persson and R. Tomás, "Improved control of the betatron coupling in the large hadron collider," *Phys. Rev. ST Accel. Beams*, vol. 17, p. 051004, May 2014.

[18] L.R. Carver, *et al.*, "Transverse beam instabilities in the presence of linear coupling in the large hadron collider," *Phys. Rev. Accel. Beams*, vol. 21, p. 044401, Apr 2018.

[19] H. Bartosik, *et al.*, "Injectors beam performance evolution during run 2," in *Proc. 2019 Evian workshop on LHC beam operation*, 30 Jan.-1 Feb. 2019.

[20] H. Damerau, *et al.*, "RF manipulations for higher brightness LHC-type beams," in *Proc. IPAC'13*, pp. 2600–2602, 12-17 May 2013 2013.

[21] M. Brugger, "R2E and availability," in *Chamonix 2014: LHC Performance Workshop*, 22-25 Sept. 2014.

[22] M. Solfaroli, *et al.*, "Combined ramp and squeeze to 6.5 TeV in the LHC," in *Proc. IPAC'16*, pp. 2039–2042, 8-13 May 2016 2016.

[23] A. Apollonio, *et al.*, "Lessons learnt from the 2016 LHC run and prospects for HL-LHC availability," in *Proc. IPAC'17*, pp. 1509–1512, 14-19 May 2017 2017.

[24] C. Schwick and B. Peterson, "LPC view on run 2," in *Proc. 2019 Evian workshop on LHC beam operation*, 30 Jan.-1 Feb. 2019.

[25] "LHC physics coordination website." https://lpc.web.cern.ch/.

[26] J.M. Jiménez, *et al.*, "Observations, analysis and mitigation of recurrent LHC beam dumps caused by fast losses in arc half-cell 16L2," in *Proc. IPAC'18*, pp. 228–231, 29 April - 4 May 2018.

[27] M. Zerlauth, *et al.*, "Operational performance of the machine protection systems of the Large Hadron Collider during run 2 and lessons learnt for the LIU/HL-

ISBN: 978-3-95450-223-3 ISSN: 2673-7000 doi:10.18429/JACoW-NAPAC2019-MOYBA1

LHC era," in *Proc. IPAC'19*, pp. 3875–3878, 19-24 June 2019 2019.

[28] A. Lechner, *et al.*, "Beam loss measurements for recurring fast loss events during 2017 LHC operation possibly caused by macroparticles," in *Proc. IPAC'18*, pp. 780–783, 29 April - 4 May 2018.

[29] L. Mether, *et al.*, "Multi-species electron-ion simulations and their application to the LHC," in *Proc. IPAC'19*, pp. 3228–3231, 19-24 June 2019.

[30] B. Salvant, *et al.*, "Experimental characterisation of a fast instability linked to losses in the 16L2 cryogenic half-cell in the CERN LHC," in *Proc. IPAC'18*, pp. 3103–3106, 29 April - 4 May 2018.

[31] H. Damerau, *et al.*, "RF manipulations for special LHC-type beams in the CERN PS," in *Proc. IPAC'18*, pp. 780–783, 29 April - 4 May 2018.

[32] D. Mirarchi, *et al.*, "Special losses," in *Proc. 2019 Evian workshop on LHC beam operation*, 30 Jan.-1 Feb. 2019.

[33] H. Burkhardt, "High-beta optics and running prospects," *Instruments*, vol. 3, no. 1, p. 22, 2019.

[34] J. Jowett, *et al.*, "The 2018 heavy-ion run of the LHC," in *Proc. IPAC'19*, pp. 3228–3231, 19-24 June 2019.

[35] J. Jowett, "Colliding heavy ions in the LHC," in *Proc. IPAC'18*, pp. 584–589, 29 April - 4 May 2018.

[36] J. Jowett, *et al.*, "The 2016 proton-nucleaus run of the LHC," in *Proc. IPAC'17*, pp. 2071–2074, 14-19 May 2017.

[37] M. Krasny, "Electron beam for LHC," *Nucl. Instrum. Methods Phys. Res. A*, vol. 540, no. 2, pp. 222 – 234, 2005.

[38] M. Krasny, "The Gamma Factory proposal for CERN." arXiv:1511.07794.

[39] M. Schaumann, *et al.*, "First partially stipped ions in the LHC ($^{208}Pb^{81+}$)," in *Proc. IPAC'19*, pp. 689–692, 19-24 June 2019.

[40] A. Abramov, *et al.*, "Collimation of partially stripped ion beams in the LHC," in *Proc. IPAC'19*, pp. 700–703, 19-24 June 2019.

[41] J. Coupard, *et al.*, ed., *LHC Injectors Upgrade, Technical Design Report*, vol. 1: Protons. Geneva, Switzerland: CERN, 2014.

[42] G. Rumolo, *et al.*, "What to expect from the injectors during run 3," in *Proc. 2019 Evian workshop on LHC beam operation*, 30 Jan.-1 Feb. 2019.

[43] S.A. Antipov, *et al.*, "Single-collimator tune shift measurements of the three-stripe collimator at the LHC," in *Proc. IPAC'18*, pp. 3036–3039, 29 April - 4 May 2018.

[44] A. Abramov, *et al.*, "Collimation system upgrades for the High Luminosity Large Hadron Collider and expected cleaning performance in run 3," in *Proc. IPAC'19*, pp. 700–703, 19-24 June 2019 2019.

[45] D. Ramos, *et al.*, "Integration of the 11 T Nb3Sn dipoles and and collimators in the LHC," *IEEE Trans. Appl. Supercond.*, vol. 26, pp. 1–5, 2016.

[46] T. Mastoridis, *et al.*, "Cavity voltage phase modulation to reduce the high-luminosity large hadron collider rf power requirements," *Phys. Rev. Accel. Beams*, vol. 20, p. 101003, Oct 2017.

[47] G. Skripka and G. Iadarola, "Beam-induced head loads on the beam screens of the inner triplets for the HL-LHC," Tech. Rep. CERN-ACC-NOTE-2018-0009, CERN, Geneva, Feb 2018.

[48] S. Kostoglou, *et al.*, "Luminosity and lifetime modeling and optimization," in *Proc. 2019 Evian workshop on LHC beam operation*, 30 Jan.-1 Feb. 2019.

[49] L.R. Carver, *et al.*, "First machine development results with HL-LHC crab cavities in the SPS," in *Proc. IPAC'19*, pp. 338–341, 19-24 June 2019.

[50] G. Iadarola, *et al.*, "Digesting the LIU high brightness beams: is this an issue for HL-LHC." Presented at the LHC Performance Workshop, Chamonix, France, 31th Jan, 2018.

[51] G. Skripka and G. Iadarola, "Beam-induced heat loads on the beam screens of the HL-LHC arcs," Tech. Rep. CERN-ACC-NOTE in preparation, CERN, Geneva.

[52] E. Todesco, "LHC energy after LS2: an update after 2018 training of sector 12." Presented at the LHC Machine Committee, CERN, Geneva, Switzerland, 6th Mar, 2019.

[53] "LHC magnet circuits, powering and performance panel website." https://mp3.web.cern.ch/.

[54] J.P. Tock, *et al.*, "The second LHC Long Shutdown (LS2) for the superconducting magnets," in *Proc. IPAC'19*, pp. 240–243, 19-24 June 2019.

[55] N. Karastathis, *et al.*, "LHC run-iii configuration working group report," in *Proc. 2019 Evian workshop on LHC beam operation*, 30 Jan.-1 Feb. 2019.

[56] F. Cerutti, "Triplet lifetime considerations." Presented at the LHC run-III Configuration Working Group meeting, CERN, Geneva, Switzerland, 30th Nov, 2018, unpublished.